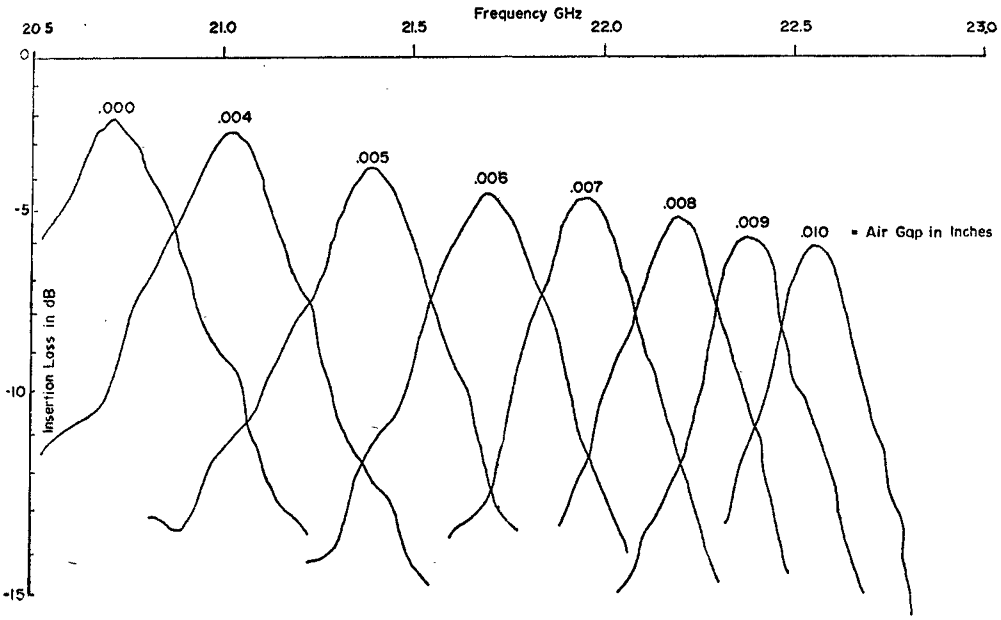

Fig. 3. Insertion loss and tuning characteristics of an experimental MILIC filter.

The tunable filter shown in Fig. 2. proved to be continuously tunable over a 3-GHz range as the air gap was increased from 0.0 to 0.022 in. The gap of 0.0 in is only approximate since the tuning mechanism did not provide for the complete elimination of all the air gap beneath the ring. Although the response could be easily tuned over the 3-GHz range, the useful tuning range due to increased insertion loss at larger gaps was about 2 GHz. This increase in insertion loss is attributed to the fact that as the gap is increased there is a decoupling of the ring from the fringe fields of the feed line. The tuning characteristic of a single resonant response for the experimental filter of Fig. 2 is presented in Fig. 3. From Fig. 3 the continuous tuning of the filter can be seen as the gap is varied from 0.0 to 0.010 in. As the air gap is increased, the resonant response is seen to tune upward in frequency as would be expected from the theoretical results [4].

III. Conclusions

The ability to mechanically tune a bandpass ring filter by varying the air gap beneath the structure provides for a continuously tunable filter for use with dielectric waveguide integrated circuits. This device could be used as a tunable preselector filter for the front end of a microwave receiver. It also provides a method for controlling the dependence of the filter response on the gap effect by providing a fine-tuning mechanism when fixed-frequency operation is desired.

Further experimental and theoretical work is necessary in order to improve the performance of the filter, particularly to decrease the insertion loss. This could be accomplished by improving the matching of the filter to the feed lines and by using a lower loss material such as alumina.

References

[1] F. S. Coale, "A traveling-wave directional filter," *IRE Trans. Microwave Theory Tech.*, vol. MTT-4, pp. 256–260, Oct. 1956.
[2] B. J. Levin and J. E. Kietzer, "Hybrid millimeter-wave integrated circuits," U.S. Army Electronics Command, Rep. ECOM-74-0577-F, Contract DAAB07-74-C-0577, Final Rep., Oct. 1975.
[3] E. A. Marcatilli, "Bends in optical dielectric guides," *Bell System Tech. J.*, vol. 48, pp. 2103–2132, Sept. 1969.
[4] P. P. Toulios and R. M. Knox, "Image line integrated circuits for system applications at millimeter wavelengths," U.S. Army Electronics Command, Rep. ECOM-73-0217-F, Contract DAAB07-73-C-0217, Final Rep., July 1974.

A New Form of Ferrite Device for Millimeter-Wave Integrated Circuits

VED P. NANDA, MEMBER, IEEE

***Abstract*—A new form for ferrite devices has been developed which finds extensive applications in the integrated circuits from *Ku* band to millimeter wavelengths. The new configuration is compatible with the emerging technology of millimeter-wave image line integrated circuits (MILIC's) which use dielectric image line as the guiding structure. Development of a MILIC isolator is discussed in detail to spotlight the salient points of the new approach. The design approach permits flexibility in layout and mechanical dimensions, and it results in low fabrication costs for MILIC ferrite devices at component and subsystem levels.**

I. Introduction

Dielectric image line [1] is emerging as an important vehicle for realizing integrated-circuit systems at millimeter waves. It is essentially a single-mode refractive waveguide which guides energy in the dielectric medium using a high-permittivity low-loss guide material laid on a metal plane. A theoretical model [2] for dielectric image guide has been developed which predicts the dispersion characteristics needed for design information of the components. The feasibility of this approach has been demonstrated by developing several passive distributed circuit components and signal processing devices. Recently, a 60-GHz communication system has been developed by IITRI for ECOM using this technology. The system description, including that for various devices, is presented by Kietzer *et al.* [3], Kaurs [4], and Shiau [5].

The use of gyromagnetic media in the dielectric image guide circuits has not been investigated so far. Since ferrite devices constitute an important building block in many RF systems, the scope of the present effort is to explore this important requirement of ferrite devices in the millimeter-wave integrated circuits. This short paper describes a few configurations of ferrite devices

Manuscript received February 24, 1976; revised June 1, 1976. This work was supported by the U.S. Army Electronics Command, Fort Monmouth, NJ 07703, under Contract DAAB07-73-C-0217.

The author was with the IIT Research Institute, Chicago, IL 60616. He is now with IITRI-ECAC, Annapolis, MD.

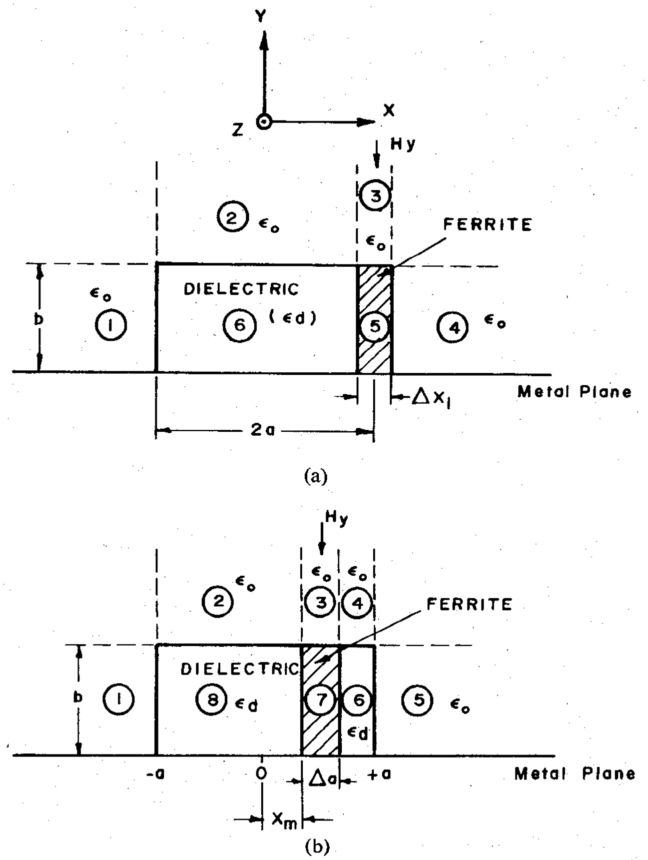

Fig. 1. Ferrite device configurations for millimeter-wave integrated circuits. (a) Edge loaded. (b) Sandwich.

compatible with the MILIC geometry. The development of a MILIC ferrite isolator is discussed in detail to spotlight the salient points of the new configuration. The MILIC ferrite devices require simple layout and therefore entail low fabrication costs compared to the conventional ferrite devices.

Two configurations for MILIC ferrite isolators are considered here. These are edge-loaded and sandwich configurations as depicted in Fig. 1. Nonreciprocity in performance can be obtained from either of the configurations. The edge-loaded configuration is simpler from analysis and fabrication considerations. The sandwich configuration, on the other hand, requires development of complex analysis. Basic theoretical considerations and results of an experimental model of an edge-loaded configuration are presented in Sections II and III.

Some of the analytic aspects of sandwich configuration are presented in [6], leading to the expression for the nonreciprocal propagation constant. The location of the circular polarization plane in the composite structure has also been derived in [6]. The sandwich configuration analysis needs to be verified experimentally. However, preliminary considerations indicate that such a configuration will have a higher figure of merit compared to the edge-loaded configuration.

II. Theoretical Concept Behind Edge-Loaded Configuration

The fundamental mode [2] for dielectric image guide of rectangular cross section is E_{11}^{y} with E_{ye} and H_{xe} as the transverse plane components. Those components extending outside the dielectric guide boundary, such as free-space regions 1–4 in Fig. 1(a), can be called the fringing fields. The E_{ye} component in

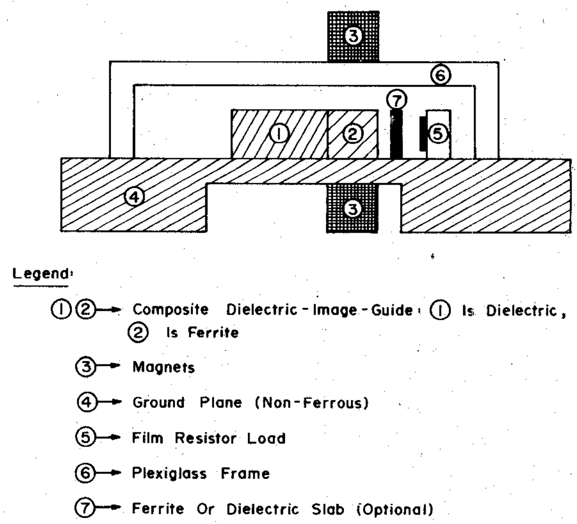

Fig. 2. MILIC ferrite isolator: typical layout.

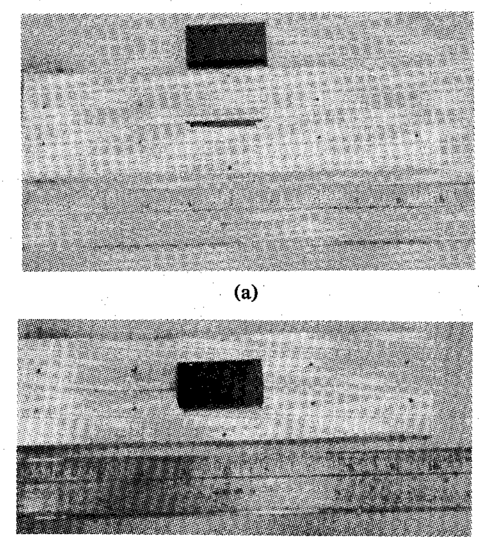

(a)

(b)

Fig. 3. Ferrite isolator in dielectric image guide configuration (*Ku* band). (a) Disassembled. (b) Assembled.

the free-space regions can be expressed as

$$E_{ye} = A_e \cos(k_y y) e^{-\alpha_x (x-a)} \cos(k_x a), \quad \text{for } x > a; \; 0 \le y \le b \tag{1}$$

and

$$E_{ye} = A_e \cos(k_x x) e^{-\alpha_y (y-b)} \cos(k_y b), \quad \text{for } y > b; \; 0 \le x \le a \tag{2}$$

where

$$A_e = \frac{k_0^2 \varepsilon_d - k_y^2}{\omega \varepsilon_0 \varepsilon_d k_z} M_1 \quad \text{amplitude term} \tag{3}$$

$\varepsilon_0, \varepsilon_d$ dielectric constants of free space and dielectric guide medium, respectively;
k_0 free-space wave number;
k_x, k_y, k_z propagation constant along the X, Y, Z axes;

$$\alpha_x = \left[\left[\varepsilon_d - \left(\frac{k_y}{k_0}\right)^2 - 1\right] k_0^2 - k_x^2\right]^{1/2} \quad \text{decay coefficient along } x \text{ axis} \tag{4}$$

$$\alpha_y = [(\varepsilon_d - 1)k_0^2 - k_y^2]^{1/2} \quad \text{decay coefficient along } y \text{ axis.} \tag{5}$$

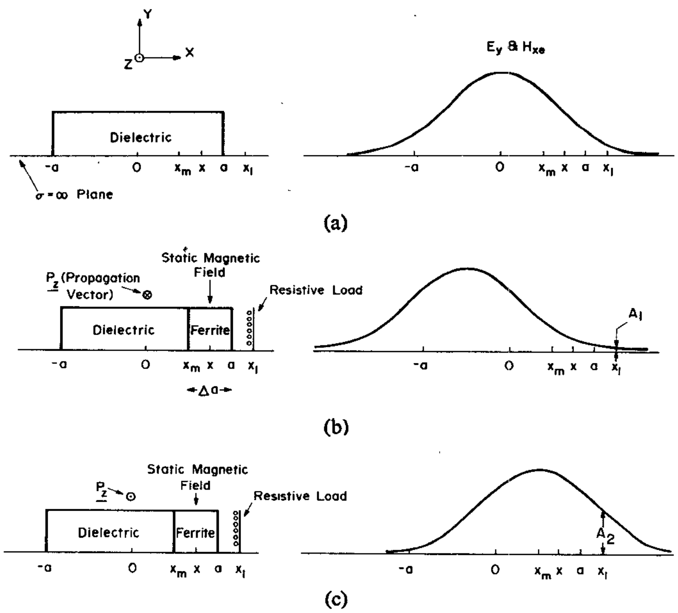

Fig. 4. Transverse field representation for various cases of edge-loaded dielectric guide. (a) Transverse field for a typical dielectric guide. (b) Transverse field for the forward-transmission case of ferrite loaded dielectric guide. (c) Transverse field for the reverse-transmission case of ferrite loaded dielectric guide.

Within the dielectric guide, the E_{ye} component is given by

$$E_{ye} = A_e \cos k_x x \cos k_y y, \qquad \text{for } -a \leq x \leq a$$
$$0 \leq y \leq b. \qquad (6)$$

It is known that the real part of permeability tensor components of an appropriately biased ferrite section takes positive and negative values of different magnitudes for two opposite directions of propagation in the structure. Therefore, amplitude (A_e) and decay coefficients (α_x,α_y) in (1) and (2) are different for the two opposite directions of propagation. This characteristic forms the basis of nonreciprocal ferrite devices using edge loading of the dielectric image guide with a ferrite slab of nominal thickness. A MILIC isolator was developed demonstrating this concept.

III. Edge-Loaded MILIC Isolator

A. General Discussion

An example demonstrating the feasibility of a new configuration of ferrite devices is the development of an edge-loaded MILIC isolator. It is discussed in detail to point out the type of approach which goes into the design of MILIC ferrite devices. Figs. 2 and 3 show the typical layout and a photograph of the edge-loaded MILIC isolator wherein the constituent parts are compatible with the MILIC goemetry and technology. The device is loaded asymmetrically which, along with ferrite behavior in terms of modifying fringing fields, leads to a pronounced nonreciprocity effect. The fringing fields interact with the nearby structures such as load, magnet, and high dielectric constant tuning slab, and this situation is used for optimizing the device performance.

The operation of the edge-loaded isolator can be described in simplified terms by considering the three cases of transverse field distribution of Fig. 4. The field amplitudes in Fig. 4(a) are in accordance with (1), (2), and (6). For the forward-transmission case of Fig. 4(b), smaller field amplitudes exist in χ_1 and χ planes. This implies lower losses, resulting from absorption and leakage, due to field interacting with film load, magnet, etc. Therefore, forward transmission has a low insertion loss. For the reverse-transmission case [Fig. 4(c)], larger field amplitudes exist in the χ_1 and χ planes. It results in a high loss or isolation. The "figure of merit" of the MILIC isolator is approximately given by the ratio of amplitudes A_2 and A_1 in the χ_1 plane.

TABLE I
Characteristics of *Ku*-Band Device

Center Frequency:	14.4 GHz
Isolation:	17.5 dB
Insertion Loss:	1.8 dB
Bandwidth:	Large
Size of Composite Guide:	1.85 in. × 0.082 in. × 0.124 in. (dielectric)
	1.85 in. × 0.082 in. × 0.041 in. (ferrite)
Ferrite Material:	Nickel-Ferrite, Trans Tech TT2-111
Tuning Slab:	1.8 in. × 0.082 in. × 0.105 in. (ferrite)
Load:	377Ω/square film resistor
Biasing Field in the Device Gap:	2000 gauss

B. Design Criteria

The design of an isolator requires knowledge of several parameters such as type of ferrite material, size of dielectric guide, filling factor of ferrite slab, strength of biasing magnetic field, and position of load. The determination of these parameters was partly done analytically and partly empirically. These details are discussed as follows.

1) Ferrite Material: The ferrite material suitable for MILIC devices, besides being of low-loss tangent ($\leq$ 0.001), should have a dielectric constant comparable to the material of the dielectric guide. This will minimize the matching problem without resorting to tapered composite structures which add to the fabrication costs. The relaxation time of the material should be comparable to the time period of interacting RF fields. The material should have an appropriate value of saturation magnetization ($4\pi M_s$). For *Ku*-band frequencies and above, a very limited choice of ferrite materials is available that meet desired parameters.

2) Size and Filling Factor of Image Guide: The cross-sectional dimensions of image guide are determined from the dispersion equations and curves in [2]. The dispersion curves relate λ_0/λ_g and $4b/\lambda_0\sqrt{\varepsilon_d}$ with aspect ratio a/b and dielectric constant ε_d as parameters. Thus dimensions (height b and width $2a$) (Fig. 1) can be calculated for the design frequency.

The filling factor is defined as the ratio of volume of the ferrite slab to the total volume of the composite structure. Its value is based on several considerations such as avoiding over moding and mismatch effects and low forward-transmission loss/guide wavelength. The height of the ferrite slab is kept the same as the dielectric guide due to simple geometry and low cost considerations. Empirically, the thickness of ferrite slab is about half its height and the length is about 45 times its thickness. In terms of demagnetization factors (N_x,N_y,N_z), it implies that for a ferrite slab of prescribed height, $N_z \leq 0.01$ and $1.6 \leq N_x/N_y \leq 1.9$ should be approximately maintained.

3) Biasing Magnetic Field: The constraints imposed on the biasing magnetic-field value are that it should operate the ferrite device away from the high loss, either due to ferromagnetic resonance effects or due to low-field effects. The resonance constraint can be checked by the Kittel equation. Furthermore, the spacing of the magnet above the ground plane should be greater than twice the height of the dielectric guide to minimize strong interaction between the magnet and the fringing RF fields.

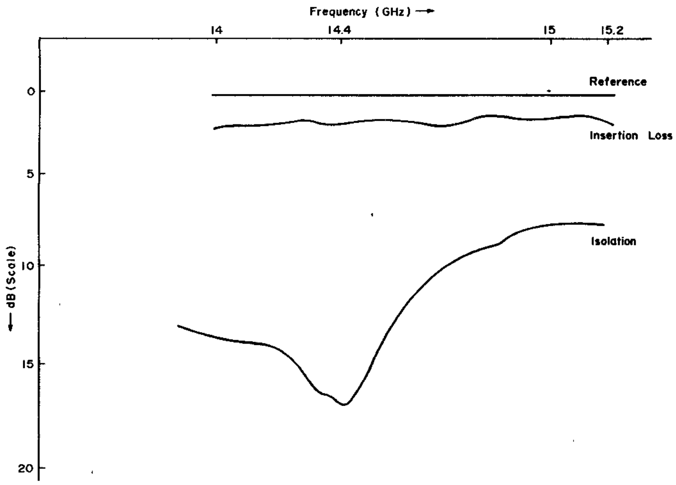

Fig. 5. *Ku*-band MILIC isolator optimized for high isolation.

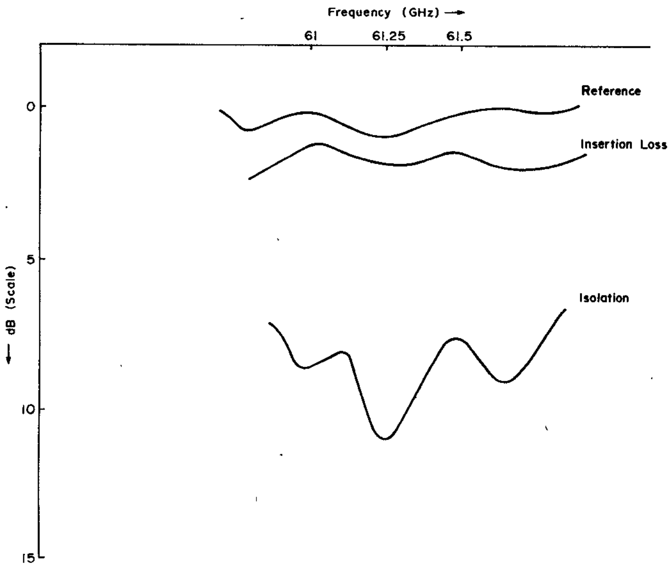

Fig. 6. *V*-band MILIC isolator.

The dimensions of magnetic pole pieces have to retain a certain form factor to supply the high biasing field. Magnet materials having high-energy product diagram (rare earth type) were mainly used.

C. Experimental Results

To verify the design concept of the edge-loaded MILIC isolator, a few devices were fabricated and tested. The initial experimental effort was carried out in *Ku* band. A figure of merit of 10 is feasible for this type of device. Table I lists the electrical and mechanical characteristics of the *Ku*-band MILIC device. Performance characteristics are shown in Fig. 5.

A MILIC isolator at *V* band was also fabricated using a configuration similar to the *Ku*-band device. The performance characteristics are shown in Fig. 6. A figure of merit of about 10 was also achieved for this band. Table II lists the electrical and mechanical characteristics of the *V*-band MILIC device.

IV. Conclusions

In this short paper, theoretical design considerations and experimental results for a ferrite isolator in the MILIC technology have been presented. The function of the device is based on the utilization of the fringe-field effect. This device constructed at 14.4 and 61.25 GHz showed an isolation of 17.5 and 11 dB, respectively. The corresponding insertion losses were 1.8 and 1.0 dB.

TABLE II
CHARACTERISTICS OF *V*-BAND DEVICE

Center Frequency:	61.25 GHz
Isolation:	11 dB
Insertion Loss:	1 dB
Bandwidth:	≈ 250 MHz between 8-dB points
Size of Composite Guide:	0.8 in. × 0.040 in. × 0.028 in. (ceramic) 0.8 in. × 0.040 in. × 0.018 in. (ferrite)
Ferrite Material:	Nickel-Ferrite, Trans Tech TT2-111
Tuning Slab:	0.8 in. × 0.040 in. × 0.02 in.
Biasing Field in Device Gap:	4400 gauss.

The concepts discussed in this short paper can lead to evolution of various other types of ferrite devices. For example, a three-port circulator can be formed by laying the edge-loaded isolator configuration in a δ-junction geometry with access ports. Among other components, a nonreciprocal phase shifter and a differential-phase-shift circulator in the MILIC geometry are also conceivable. With various adaptations of these forms, several ferrite device applications can be realized. It is estimated that a ferrite device using sandwich configuration will have a higher figure of merit compared to the edge-loaded configuration. Ferrite devices in MILIC geometry have the advantage of being compact and of low cost compared to the ferrite devices in conventional structures.

References

[1] "Image line integrated circuit for system applications at millimeter wavelengths," Final Report, Contract DAAB07-73-C-0217 to IIT Research Institute, Chicago, U.S. Army Electronics Command Report ECOM-73-0217-F, July 1974.
[2] R. M. Knox and P. P. Toulios, "Integrated circuits for the millimeter through optical frequency range," Proc. Symposium on Submillimeter Waves, Polytechnic Institute of Brooklyn, N.Y., March 31–April 2, 1970.
[3] J. E. Kietzer, A. R. Kaurs, and B. T. Levin, "A *V*-band communication transmitter and receiver system using dielectric waveguide integrated circuits," this issue, pp. 797–803.
[4] A. R. Kaurs, "A tunable bandpass ring filter for rectangular dielectric waveguide integrated circuits," this issue, pp. 875–876.
[5] Y. Shiau, "Dielectric rod antennas for millimeter-wave integrated circuits," this issue, pp. 869–872.
[6] "Hybrid millimeter wave integrated circuits," Final Rep., Contract DAAB07-74-C-0577 to IIT Res. Inst., Chicago, IL, U.S. Army Electronics Command Rep. ECOM-74-0577-F, Oct. 1975.

The Fabrication of Dielectric Image Lines Using Casting Resins and the Properties of the Lines in the Millimeter-Wave Range

KLAUS SOLBACH

***Abstract*—Experiments with dielectric image lines fabricated of casting resins are described, and the properties of the electromagnetic fields and the phase coefficients of the waves in the millimeter-wave range (26–40 GHz) are discussed. As an example, a ring resonator and the measurement of its insertion loss is presented.**

Manuscript received February 11, 1976; revised May 6, 1976.
The author is with the Lehrstuhl für Allgemeine und Theoretische Elektrotechnik, University of Duisburg, West Germany.